2018-07

WEC Design Based on Refined Mean Annual Energy Production for the Israeli Mediterranean Coast

Stuhlmeier, Raphael

10.1061/(ASCE)WW.1943-5460.0000451
Journal of Waterway, Port, Coastal, and Ocean Engineering
American Society of Civil Engineers

WEC design based on refined mean annual energy production for the Israeli Mediterranean coast*

Raphael Stuhlmeier and Dali Xu

Abstract

Using the Israeli Mediterranean as an example, we address the impact of resource variability and device survivability on the design of floating-body wave-energy converters (WECs). Employing a simplified heaving-cylinder as a prototypical WEC, several device sizes, corresponding to the most frequently encountered and most energetic sea-states in the Israeli Mediterranean, are investigated. Mean-annual energy production is calculated based on the scatter-diagram/power-matrix approach. Subsequently, a measure for significant device motions under irregular sea-states akin to the spectral significant wave-height is developed, and cut-offs to regular operation are explored from the perspective of these significant displacements. The impact of this WEC down-time is captured in a refinement of mean-annual energy production, which consists of supplementing the scatter-diagram/power-matrix calculations by a Boolean displacement matrix. In the Israeli Mediterranean, where most of the annual incident wave power comes in infrequent winter storms, larger WECs outperform smaller WECs by a greater margin when down-time is taken into account. Analogous displacement cut-offs for refining calculations of mean-annual energy production may inform WEC design for other sites.

1 Introduction

The commercial harvesting of power from ocean waves via floating bodies remains a current challenge despite decades of theoretical and experimental work, not least because of the high variability of the underlying resource. Floating body wave-energy converters (WECs) are constrained in size by the lengths of the usually encountered waves, and must be small enough to undergo significant displacements in typically encountered sea-states. Competing with this is the need to ensure that devices are robust enough to survive the strains of the marine environment, including higher-energy seas associated with storms that will inevitably be encountered over the lifetime of a converter, which may be as long as 25 years Starling (2009).

The performance of wave-energy converters (WECs) is commonly measured by calculating the mean annual energy production (MAEP). Given a WEC design, this entails calculating an $N \times M$ table of the captured power with entries indexed by significant wave–height H_s and energy period T (called a *power matrix*), and multiplying this matrix entry-by-entry with an $N \times M$ matrix giving the annual frequency of occurrence of each sea-state (called a *scatter diagram*). The sum of all

*Published in **Journal of Waterway, Port, Coastal, and Ocean Engineering**, Volume 144, Issue 4 doi.org/10.1061/(ASCE)WW.1943-5460.0000451

entries of this product then yields the MAEP, which assumes that the device operates continuously throughout the year.

The intention of the present investigation is to examine WEC design from the perspective of MAEP while taking into account device motions, thereby refining the classical matrix approach (see Hiles et al. (2015)). This is presented using wave-climate data from the Israeli Mediterranean as a case study. The natural variability of the wave-power resource off Israel's coast impacts design in a complex manner: while larger devices may produce more during relatively infrequent, high-energy storms with H_s up to 5 m, they may fail to produce power during common summer conditions where H_s is less than 1 m. In addition, a more realistic appraisal demands that device motions must be constrained to ensure device survival, which reduces the average operational time, and thereby the true MAEP. To account for this, we supplement the scatter diagram and power matrix with a new displacement matrix, that records WEC displacement for values of H_s and T. By introducing a cut-off value the displacement matrix may be converted to a Boolean matrix, and the MAEP calculated by term-wise multiplication thereof with the scatter diagram and power matrix, and subsequent summation. This adds a simple measure of WEC downtime to calculations of MAEP, and allows for a novel assessment of device design based on such criteria.

In what follows, we shall first outline the background of the floating, cylindrical WEC considered here as a model. Subsequently, we present the wave climate based on measurements off the coast of Ashdod, Israel. Therein, four classes of sea-state are identified based on ranges of significant wave-height, and their contribution to the annual incident wave power is illuminated. On the basis of these classes, three different device designs are considered for both classical MAEP calculations as well as the new refined MAEP based on device downtime for large displacements. Finally, we present conclusions together with design recommendations. Two appendices contain scatter diagrams, power matrices and displacement matrices for each of the three designs.

2 The floating cylinder WEC

The vertically floating cylinder is a natural model for a floating wave energy converter, whose study goes back at least to Berggren & Johansson's 1992 examination of two floating, axisymmetric cylinders oscillating in heave. More recent studies employing floating cylinders as WECs have been made by Garnaud and Mei 2009, Child and Venugopal 2010, Borgarino et al 2012, Teillant et al 2012, Wu et al 2014, and many others. The ease of solving the Laplace equation in cylindrical coordinates allows for an analytical treatment, first explored in work by Black & Mei 1970, and has allowed for a wealth of insight into the hydrodynamics of such a device. Floating cylindrical bodies are also found in current commercial WEC technologies, such as the Carnegie Wave Energy CETO device.

The focus of the present work is on device size as a function of MAEP and survivability considerations, rather than on the development of a novel WEC design. Consequently, the geometry and basic parameters of the cylindrical WEC are pared down to the essentials, and are depicted in Figure 1.

The Oxy plane is the still water surface and the z-axis points upwards. The cylinder is submerged to a draft q in deep water of depth h (for computations $h = 200$ m is used), and chosen with a radius q, and damping coefficient d representing a power take-off (PTO) which extracts energy from the heave motion of the cylinder. This PTO of constant characteristic assumes that the electrical power generated is equal to the mechanical power absorbed by the WEC. In this simplified framework, the design of the cylindrical WEC is reduced to determining the two parameters q and d.

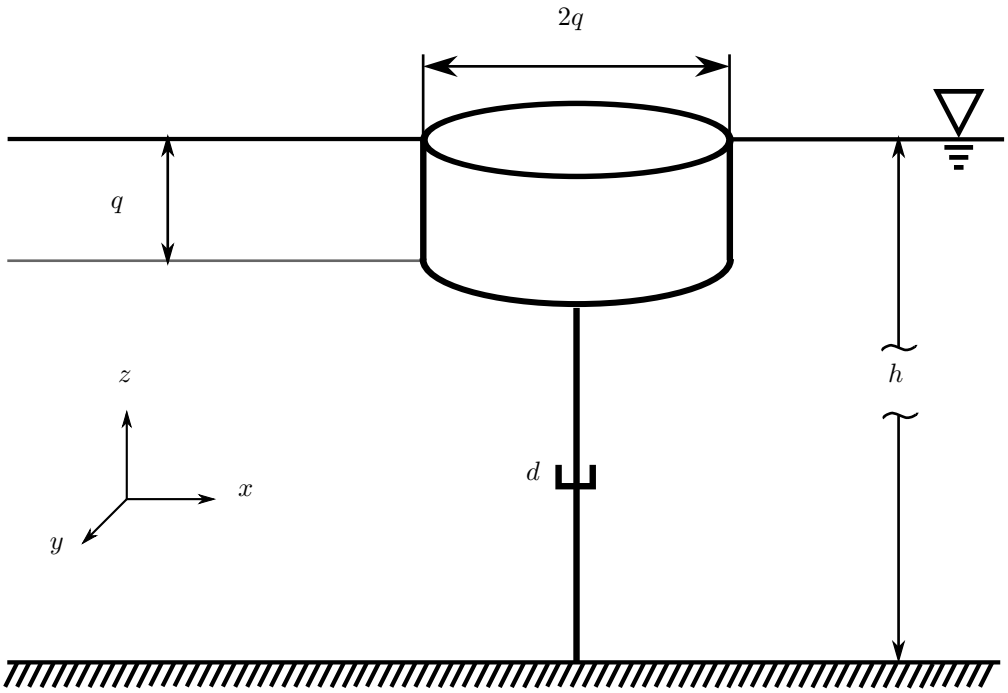

Figure 1: Schematic geometry and parameters of the floating vertical cylinder WEC, with draft q, diameter $2q$, damping d, in water of depth h.

3 Wave power on the Israeli Mediterranean coast

The wave climatology of the Israeli Mediterranean coast is highly seasonal, with the winter months exhibiting high waves and a "storm-wave" climate, while the summer months are characterized by a low to intermediate "swell-wave" climate Goldsmith and Sofer (1983). To investigate the design and subsequent performance of WECs, in Appendix A we present scatter diagrams for deep water off the Israeli coast, based on the report Kroszynski and Stiassnie (1978). These comprise an annual scatter diagram, a winter (October to March, inclusive) scatter diagram, and a summer (April to September, inclusive) scatter diagram, giving frequency of occurrence of sea-states indexed by energy period T and significant wave–height H_s. Since the point-absorber to be considered is axisymmetric, the scatter diagrams and resulting data are presented without regard to the incident wave direction.

The annual scatter diagram (Figure 3) is recast in a more accessible form, along the lines of Kroszynski and Stiassnie (1979), and the condensed data presented in Table 1. This will form the basis for our WEC design. Within the classes defined in Table 1, more than 90% of the periods fall in the following ranges: 3–6 s (Class 1), 4–9 s (Class 2), 7–11 s (Class 3), and 9–12 s (Class 4).

The average annual wave energy flux per meter wave-front may be calculated from the scatter

Class	Description	Range of H_s (m)	Freq. occurrence (%)	Rel. contribution (%)
1	Calm sea	< 1	60	7.7
2	Stormy sea	$1 - 3$	34.6	42.3
3	Very stormy sea	$3 - 5$	4.9	39.4
4	Extremely stormy	≥ 5	0.5	10.6

Table 1: Classification of sea states off the coast of Israel by range of significant wave heights H_s (m). Given are the annual frequency of occurrence of each class, and the relative contribution to the average power, both in percent.

diagram (Figure 3, Appendix A) by summing over all energy fluxes F_{ij}, where

$$F_{ij} = \frac{\rho g^2}{64\pi} T_j H_i^2, \tag{1}$$

$i \in \{0, \ldots, 8.5\}$, and $j \in \{3, 4, \ldots, 13\}$ range over the significant wave-height H_s and energy period T, respectively. Equation (1) is strictly accurate only for T_j equal to the spectral energy period. Otherwise transformations from peak or mean period, based on the spectral shape, must be employed (see Arena et al. (2015)).

This yields 7.9 KW of energy flux per meter wave front in the annual average, with a summer average of 4.4 KW/m and a winter average of 11.6 KW/m. Table 1 further illustrates the significant variability involved in this resource, with calm conditions predominating 60% of the year, while the major contributions to the annual energy budget occur during infrequent stormy events. Indeed, very stormy seas of class three occur less than 5% of the time (about 18 days per year), but contribute nearly 40% to the annual wave-power budget. Related to this is the issue of extreme waves and their impacts on the feasibility of WEC designs. An analysis of the data based on the Weibull distribution Rosen and Kit (1982) shows a two year return period for a significant wave height H_s of 5.6 m, and 10 and 20-year return periods for H_s of 7 and 7.5 m, respectively.

It is not evident how a WEC should be designed with this variability in mind. A WEC designed to operate well in Class 3 may be ill suited to conditions of Class 1 or 2, and vice versa. To this end, three WEC designs will be considered, each operating preferentially in an averaged state for Class 1, 2, or 3 (Class 4 sea-states occur on less than two days per year on average, and do not contribute significantly to the overall annual energy production; no WEC design for such seas is considered). These average states for the WECs of Class 1, 2 and 3, calculated from the data of Figure 3, are given in Table 2, and used as a guideline for WEC design.

4 WEC design for Israeli Mediterranean coasts

As mentioned in the previous Section, three designs are considered, and summarised in Table 3. Each design is tuned to perform optimally for a design period T as given in Table 2. The design procedure – choosing the buoy size such that its resonance frequency coincides with this design period – has been detailed elsewhere Xu et al. (2017); Garnaud and Mei (2010).

Class	Average Period (s)	Average H_s (m)
1	4.8	0.6
2	7.2	1.6
3	9.2	3.8
4	11.1	5.8

Table 2: The averaged energy period T and averaged significant wave–height H_s for each of the four classes of Table 1.

Class	Radius (m)	Damping (Ns/m)
1	3.7	20589
2	8.4	170481
3	13.7	579115

Table 3: Characteristics of WECs designed for operation in Class 1, 2, or 3. Given are radius (equal to draft) and damping coefficient for the floating vertical cylinder (see Figure 1).

A comparison of the absorbed power by each of the three device designs, as a function of wavenumber k, is given in Figure 2. As expected for a floating cylinder, the bandwidth of each device is rather narrow. The peak power absorption for WEC designs 1, 2 and 3 are 104.1 KW, 353.7 KW, and 737.6 KW, respectively, for an incident wave of unit amplitude ($a_0 = 1$ m).

4.1 Power capture and significant displacement

For a given device and a variance-density spectrum $S(k)$, where k denotes the wavenumber, the total absorbed power is

$$P_a^{\text{total}} = \int_0^\infty 2P_a^*(k)S(k)dk. \tag{2}$$

where P_a is the dimensional absorbed power, a_0 the incident wave amplitude, and P_a^* is the absorbed power per unit incident wave amplitude squared, i.e. $P_a^* = P_a/a_0^2$. Equation (2) is used to calculate the power matrices given in Appendix B, more details of which are provided therein.

We address device survival by calculating the *significant motions* that may be encountered by a floating-cylinder WEC for a given incident spectrum. Unlike for a monochromatic wave, where the displacement response of the WEC may be calculated explicitly, in irregular waves it is no longer possible to directly define a displacement without reverting to a time-domain analysis based on realizations of the sea-surface.

However, just as the spectrum describes the distribution of wave energy among different frequencies, and allows for statistical inferences, such as a definition of the significant wave-height, so

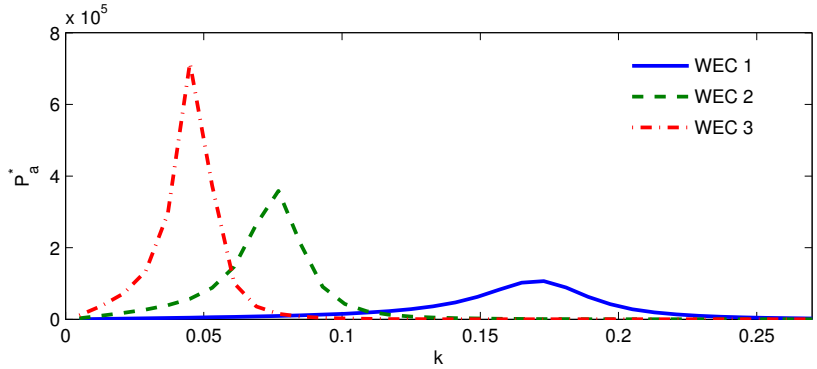

Figure 2: Comparison of absorbed power per unit incident wave amplitude squared P_a^* (W) as a function of wavenumber k for the three WEC designs considered, for an incident wave of unit amplitude ($a_0 = 1$).

analogously we may consider a *displacement spectrum* (see Xu et al. (2017))

$$E_z(k) \equiv S(k)(\tilde{a}_z)^2, \tag{3}$$

where $\tilde{a}_z$ is the relative amplitude of the heave displacement, and thereby define the *significant displacement* by

$$\zeta^{1/3} = 4 \cdot \left(\int_0^\infty E_z(k) dk \right)^{1/2}. \tag{4}$$

Here $\zeta^{1/3}$ is the the distance from the trough to the crest of the displacement. We emphasize that these displacements are not the extremes of the vertical travel, but represent significant displacement analogous to the significant wave-height.

5 Results

5.1 Classical mean annual energy production

The scatter diagram presented in Appendix A and the power matrices of Appendix B enable immediate calculation of the MAEP for Israeli waters via entry-wise multiplication, the results of which are presented in Table 4. These results present a departure from what might be expected purely on the basis of the sea-state classification (Table 1). While Class 2 presents the overall largest relative contribution to annual wave energy, it is the device designed for Class 3 that shows the largest MAEP by classical methods. Indeed, the smallest device produces nearly 80% of its energy during sea-states of Class 1 and 2. In contrast, the largest device, while producing nearly 55% during the Class 3 sea-states for which it is designed, gains nearly 15% of its annual energy production (AEP) from extremely stormy conditions of Class 4 (compared to 6% for the intermediate device, and less than 3% for the smallest). These results are summed up in Table 5.

An interesting picture emerges when the seasonality of the wave resource is considered explicitly. Table 7 in Appendix A, analogous to Table 1, sums up the data of the winter and summer scatter

WEC Design	Radius (m)	MAEP (W)
1	3.7	$6.039 \cdot 10^3$
2	8.4	$2.495 \cdot 10^4$
3	13.7	$3.272 \cdot 10^4$

Table 4: Mean annual energy production (MAEP) in W for WECs designed for operation in Class 1, 2, or 3.

Sea-state	WEC 1	WEC 2	WEC 3
Class 1	18.1	4.2	1.2
Class 2	58.2	49.2	30.6
Class 3	21.0	40.4	54.2
Class 4	2.7	6.1	14.0

Table 5: Percentage contributions of different sea-states (Class 1, 2, 3, and 4) to AEP for the three WEC designs considered (WEC 1, 2, and 3). Entries are given in (%), and the sum over each column is 100%.

diagrams. For summer conditions, where H_s of less than 1 m prevails more than 63% of the time, the Class 2 device exhibits an AEP of $1.5 \cdot 10^4$ W, outperforming both the smaller Class 1 device ($5.0 \cdot 10^3$ W) as well as the larger Class 3 device ($1.2 \cdot 10^4$ W), at odds with the picture for overall AEP. In winter conditions, the AEP of the Class 3 WEC ($5.4 \cdot 10^4$ W) further outstrips that of Class 1 ($7.1 \cdot 10^3$ W) and Class 2 ($3.6 \cdot 10^4$ W).

5.2 Refined mean-annual energy production: survival mode in severe seas

The above data for MAEP should be refined further by taking into account limits on device motions, which will dictate when a given device must cease operation and be placed in survival mode. One may anticipate, for example, that a small device designed for Class 1 seas would cease operating in extremely stormy conditions of Class 4, so that this 2.7% contribution to MAEP in Table 5 would be lost.

While it has been possible to base the foregoing analysis on purely hydrodynamic considerations, there is at present no widely accepted nor implemented survival mode to protect floating-body WECs when normal operating conditions are exceeded Coe and Neary (2014); Peckolt et al. (2015). The existing literature largely suggests strict cut-offs based only on H_s, rather than device response Maisondieu (2015); Hiles et al. (2016). Consequently, the choice of a cut-off is necessarily somewhat arbitrary, and should be understood as an illustrative refinement of the MAEP rather than a strict limit.

The design procedure of each of the three converters is such that the displacement (and power

capture) is maximal at the periods given in Table 2. Under such conditions, the undamped floating cylinder is in resonance with the incident waves. In each of Classes 1 to 3 the damping is chosen to maximize power capture at this resonance period, resulting in a relative amplitude of the structure's displacement normalized by incident wave height, ζ/a_0, close to 2.4.

One important check on WEC motions is that the device never leaves the water surface: hence, for a device displacement amplitude ζ and a wave amplitude a_0, we require $\zeta - a_0 < q$ for q the device draft. Since the maximum value of $\zeta = 2.4a_0$ in each case, this means that the device displacements should in any case be limited to 1.7 times the draft, or 6.3 m for Class 1, 14.3 m for Class 2, and 23.3 m for Class 3. Imposing only this restriction on the significant device motion leaves the MAEP essentially unchanged (see Figure 9, Figure 10 and Figure 11 in Appendix B), and also exposes the smaller devices to sea-states far beyond their design conditions.

5.2.1 Displacement cut-offs for cessation of power production

Any number of cut-off criteria may be imposed beyond which the WEC in question may be assumed to be in survival mode. One simple possibility is to limit the significant amplitude of the displacement $\zeta^{1/3}$ under a JONSWAP spectrum to the device draft. We term this cut-off A, and data on the resulting refined MAEP (rMAEP) is given in Table 6.

Under ideal, design conditions, namely monochromatic waves of period 4.8 s, a WEC of Class 1 undergoes displacements equal to 2.4 times the incident wave amplitude. The design specification from Table 3 foresees a height of 0.6 m, so that we expect a total vertical travel under these conditions of $\zeta_{\text{design}} = 1.5$ m. Similarly, the expected vertical travel for a Class 2 WEC is $\zeta_{\text{design}} = 3.8$ m, and for a Class 3 WEC we expect a travel of $\zeta_{\text{design}} = 9$ m. A further possibility for a cut-off is to limit device motions to 150% (called cut-off B) or 200% (called cut-off C) of these designed–for motions, e.g. for cut-off C, displacements in Figure 9 (which shows $\zeta^{1/3}$ for a Class 1 WEC) should not exceed 3 m.

Introducing these cut-offs, each of the displacement matrices in Table 9, Table 10 and Table 11 may be reduced to a Boolean matrix, where entries in excess of the cut-off are replaced by 0 and those below the cut-off replaced by 1. A calculation of the rMAEP consists of multiplying the scatter diagram, power matrix, and Boolean displacement matrix entry-by-entry and summing, the results of which are presented in Table 6, where they are termed rMAEP A, B, and C for cut-offs A, B and C, respectively.

WEC Design	Draft (m)	rMAEP A (W)	rMAEP B (W)	rMAEP C (W)
1	3.7	$4.2 \cdot 10^3$	$2.2 \cdot 10^3$	$3.3 \cdot 10^3$
2	8.4	$2.4 \cdot 10^4$	$1.8 \cdot 10^4$	$2.4 \cdot 10^4$
3	13.7	$3.3 \cdot 10^4$	$3.3 \cdot 10^4$	$3.3 \cdot 10^4$

Table 6: Refined mean annual energy production (rMAEP) in W for WECs designed for operation in Class 1, 2, or 3, with cut-offs for survival mode. rMAEP A assumes a displacement $\zeta^{1/3} < q$. rMAEP B assumes a displacement $\zeta^{1/3} < 1.5\zeta_{\text{design}}$. rMAEP C assumes a displacement $\zeta^{1/3} < 2\zeta_{\text{design}}$.

It is immediate that the smaller devices suffer most when constraints on device motion are imposed. The largest WEC, designed for very stormy seas, need scarcely cease operation based on

the cut-off criteria imposed, and outperforms the two smaller designs by an even wider margin than when a classical measure of MAEP is employed. Indeed, even imposing a uniform cut-off of ≥ 3.5 m of vertical travel for all devices, the largest device continues to outperform the smaller designs.

6 Conclusions

The intention of the present work is to use the Israeli Mediterranean as case study for WEC design. Significant wave–heights typically range from less than 1 m in the summer months, to more than 3.5 m during winter storms. We have proposed to address the following questions: (i) from the perspective of mean annual energy production, is it preferable to design a larger structure for more energetic, infrequent events, or a smaller structure for continuous operation during low energy sea–states? (ii) What displacements may be expected of a structure over a typical year of operation, and how might survival modes for seas outside the intended operating conditions impact yearly power absorption? (iii) What yearly power production can be expected from floating–cylinder WECs deployed in deep water off Israel's coast?

Three sizes of point absorber have been proposed to exploit the wave-power resources of the Israeli Mediterranean, suited respectively for frequent, calm seas; intermediate, stormy seas; and less frequent, high-energy, extremely stormy seas. Accordingly, these devices range from smaller to larger, and have disparate capacities to absorb energy from sea-states outside of their operating range.

The Israeli coast provides an annual average energy flux of 7.9 KW per meter wave front, with much of this contributed by winter storms. Three sizes of bottom-referenced, heaving cylinder WECs, with radii of 3.7 m, 8.4 m, and 13.7 m were used to assess the potential for capturing wave power. Classical computations using a scatter diagram and power matrices yield a MAEP of 6.0, 25.0 and 32.7 KW, respectively.

Numerous factors may ultimately influence the survival of a wave-energy converter, including the corrosive effects of the marine environment, biofouling, and other factors that are not readily captured by purely hydrodynamic considerations. In addition, WEC survival will need to be considered in light of extreme loads due to very steep waves (see Boccotti (2014)). Employing time-domain models Hiles et al. (2016), and taking into account the statistics of high waves and the forces associated with their impacts on marine structures Fedele and Arena (2005); Arena (2005); Romolo and Arena (2008); Boccotti et al. (2012) will allow for a more holistic, albeit computationally demanding, perspective on WEC survival than considered here.

We have proposed a new and fast measure of MAEP that takes into account device down-time, by means of a cut-off for device displacement. A "displacement matrix" may be calculated akin to the power matrix, giving significant displacements for an array of spectral sea-states. Subsequently, this matrix may be converted to a Boolean matrix by employing a cut-off for vertical travel, beyond which the WEC must cease operation and enter survival mode. A refined MAEP may then be calculated by entry-by-entry multiplication of the power matrix, scatter diagram, and Boolean displacement matrix.

As one illustrative case, we have introduced a vertical travel cut-off equal to either 1.5 or 2 times the vertical travel for which each device type is designed. We find that such a measure disproportionately impacts smaller devices, for which the resulting MAEP is significantly reduced. For this case study using Israeli Mediterranean wave data, we may conclude that (i) larger devices (tuned to less frequent, higher-energy sea-states) are preferable to smaller devices, and (ii) that this advantage becomes more pronounced when device survivability is taken into account.

The economic viability of such large devices is one issue which may serve to complicate any analysis of WEC design, and as ultimate survival will likely depend on extreme loads and fatigue analysis, a final determination must be made with the specifics of a device in-hand. A further complication is introduced by the seasonality of the wave-power resource: while the Class 3 design is clearly superior in terms of MAEP, it is scarcely able to produce power from the calm sea states that predominate 60% of the time. Such intermittency in power production may pose a problem for the power grid, and highlights an additional hurdle in site-selection as well as WEC design.

It is to be hoped that the proposed refinement to the traditional method of calculating MAEP may be used by other practitioners, and draw attention to the demands of WEC survival as a crucial element of design. For a given design, a maximum displacement may be established (in either a single degree of freedom, or in several with appropriate weighting of each), or else a displacement cut-off may be developed *ad hoc* to evaluate WEC designs. This adds another important element to the current approach of determining mean annual energy production Kofoed and Folley (2016), while being fast and straightforward to implement.

A Scatter Diagrams for the Israeli Mediterranean

This appendix provides the scatter diagrams for the Israeli Mediterranean. The annual average is given in Figure 3, the summer average is given in Figure 4, and the winter average in Figure 5. This data is recast in table form in Table 7, which is a seasonal breakdown (winter/summer) of Table 1 based on the scatter diagrams (Figure 4 and Figure 5).

Class	H_s (m)	Freq. occurrence (%)		Rel. contribution (%)	
		Winter	Summer	Winter	Summer
1	< 1	56.5	63.4	4.5	15.6
2	$1 - 3$	34.2	35.0	33.6	64.9
3	$3 - 5$	8.4	1.5	47.4	19.4
4	≥ 5	0.9	0	14.4	0

Table 7: Classification of summer and winter sea states off the coast of Israel by range of significant wave heights H_s (m). Given are the frequency of occurrence of each class, and the relative contribution to the average power, both in percent.

B Power and displacement matrices

This appendix gives the power matrices for WECs of Class 1, 2 and 3 in Figure 6, Figure 7 and Figure 8, respectively. Also given are the analogous displacement matrices (showing the significant amplitudes of displacement, eq. (4)) of WECs of Class 1, 2 and 3 in Figure 9, Figure 10 and Figure 11.

The power matrices are calculated using (2) for all three WEC designs (see Figure 2), where the variance density spectrum employed is a JONSWAP spectrum with peak period T_p and significant

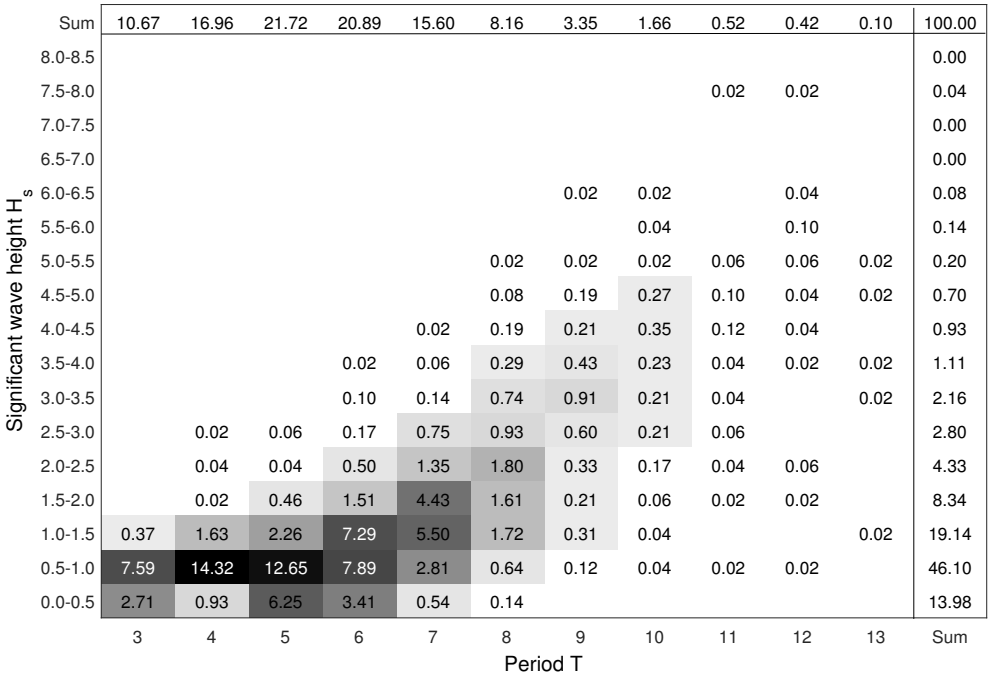

Figure 3: Annual average scatter diagram for the Israeli Mediterranean coast based on observations in deep-water off the coast of Ashdod, Israel. The vertical shows significant wave–height (from 0 to 8.5 m), and the horizontal the energy period (from 3 to 13 seconds), while the entries give an annual percentage of occurrence.

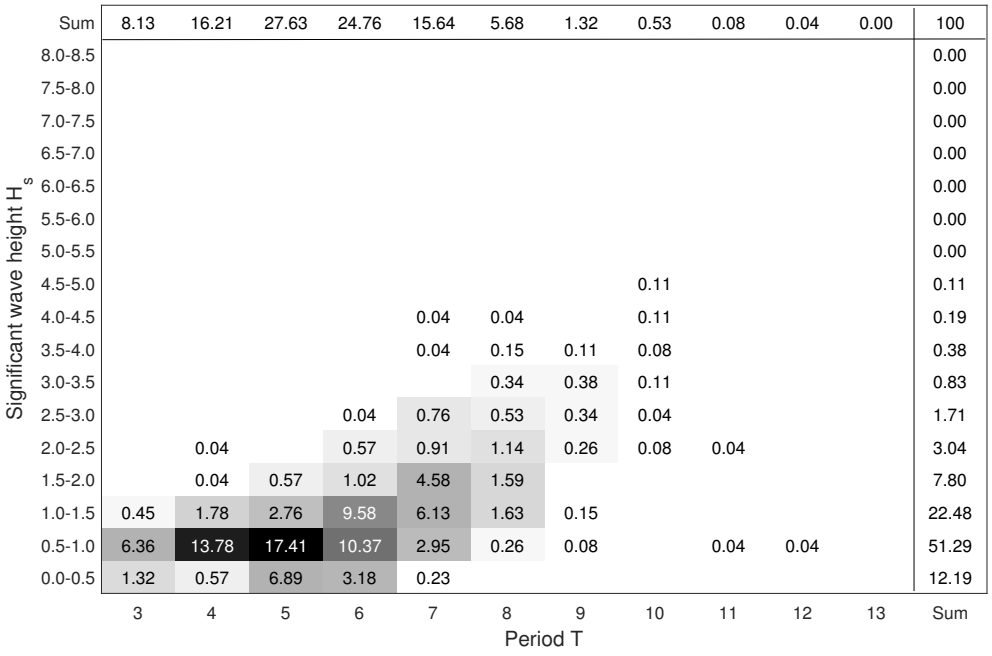

Figure 4: Summer (April to September, inclusive) average scatter diagram for the Israeli Mediterranean coast based on observations in deep-water off the coast of Ashdod, Israel. The vertical shows significant wave–height (from 0 to 8.5 m), and the horizontal the energy period (from 3 to 13 seconds), while the entries give an annual percentage of occurrence.

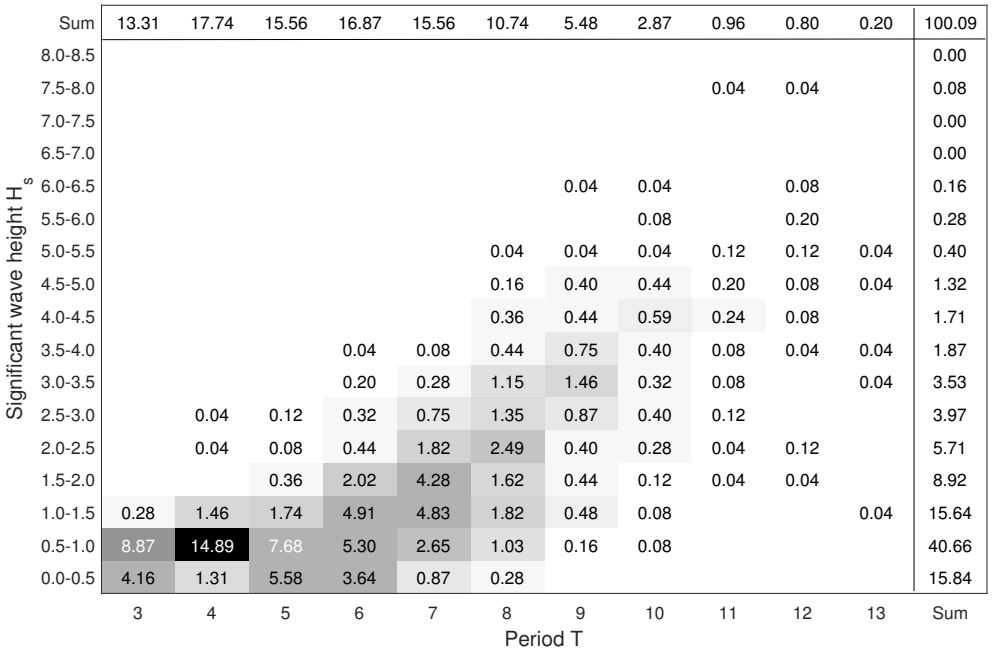

Figure 5: Winter (October to March, inclusive) average scatter diagram for the Israeli Mediterranean coast based on observations in deep-water off the coast of Ashdod, Israel.The vertical shows significant wave–height (from 0 to 8.5 m), and the horizontal the energy period (from 3 to 13 seconds), while the entries give an annual percentage of occurrence.

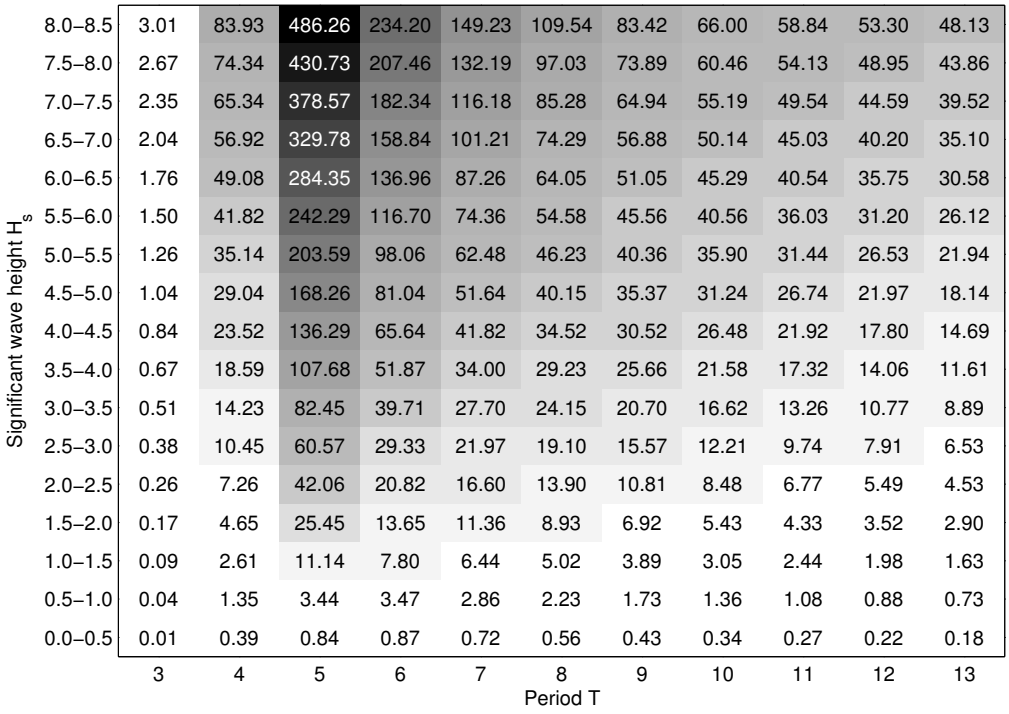

Figure 6: Power matrix for a WEC designed to operate in Class 1. The vertical shows significant wave–height (from 0 to 8.5 m), and the horizontal the energy period (from 3 to 13 seconds), while the entries give absorbed power (KW).

wave-height H_s of the corresponding bin. The peakedness parameter γ is adjusted based on T_p and H_s using WAFO Brodtkorb et al. (2000).

Acknowledgements

RS was supported by Israel Science Foundation Grant 464/13. The authors would like to thank Prof. Michael Stiassnie for helpful discussions and comments on the manuscript.

References

Arena, F. (2005). "On non-linear very large sea wave groups." *Ocean Engineering*, 32(11-12), 1311–1331.

Arena, F., Laface, V., Malara, G., Romolo, A., Viviano, A., Fiamma, V., Sannino, G., and Carillo,

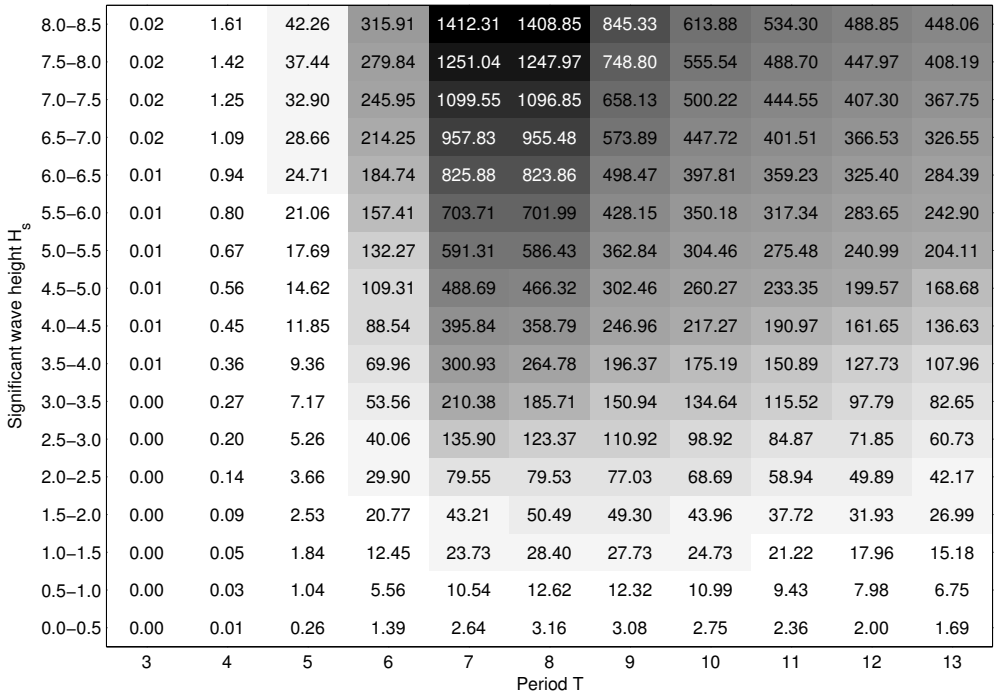

Figure 7: Power matrix for a WEC designed to operate in Class 2. The vertical shows significant wave–height (from 0 to 8.5 m), and the horizontal the energy period (from 3 to 13 seconds), while the entries give absorbed power (KW).

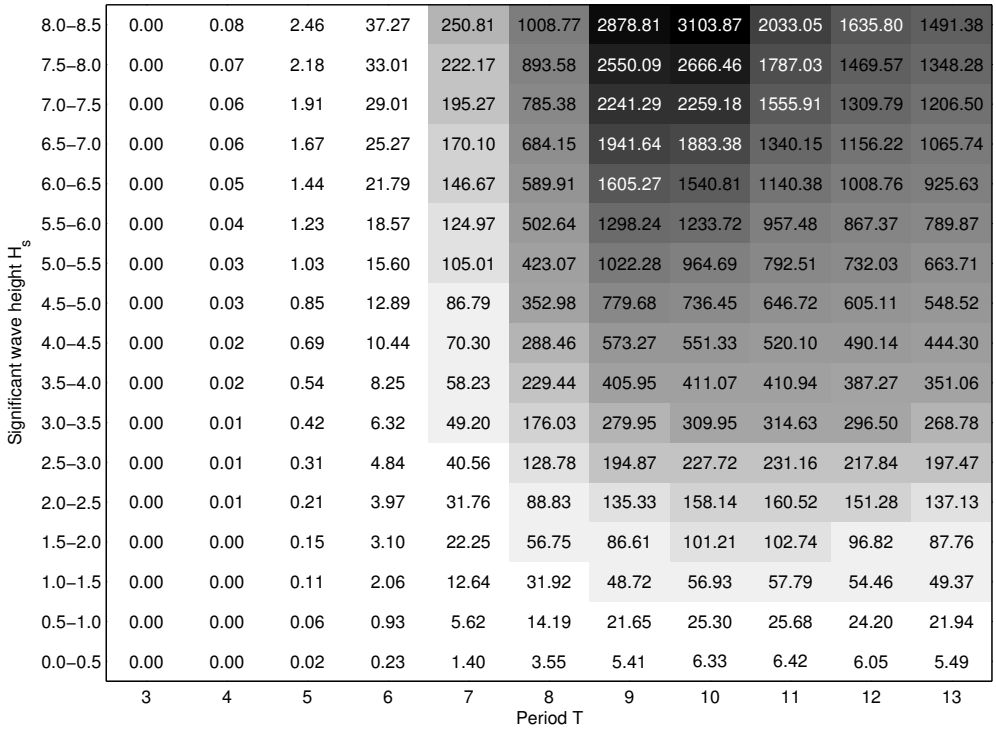

Figure 8: Power matrix for a WEC designed to operate in Class 3. The vertical shows significant wave–height (from 0 to 8.5 m), and the horizontal the energy period (from 3 to 13 seconds), while the entries give absorbed power (KW).

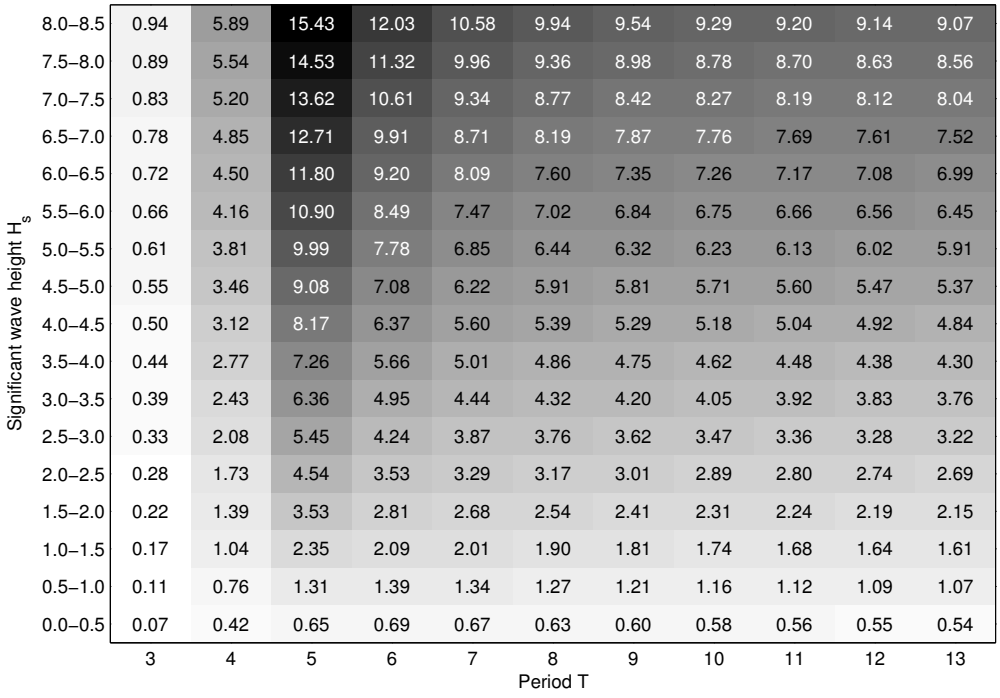

Figure 9: Displacement matrix for a WEC designed to operate in Class 1. The vertical shows significant wave–height (from 0 to 8.5 m), and the horizontal the energy period (from 3 to 13 seconds), while the entries give the significant displacement $\zeta^{1/3}$ in heave in m.

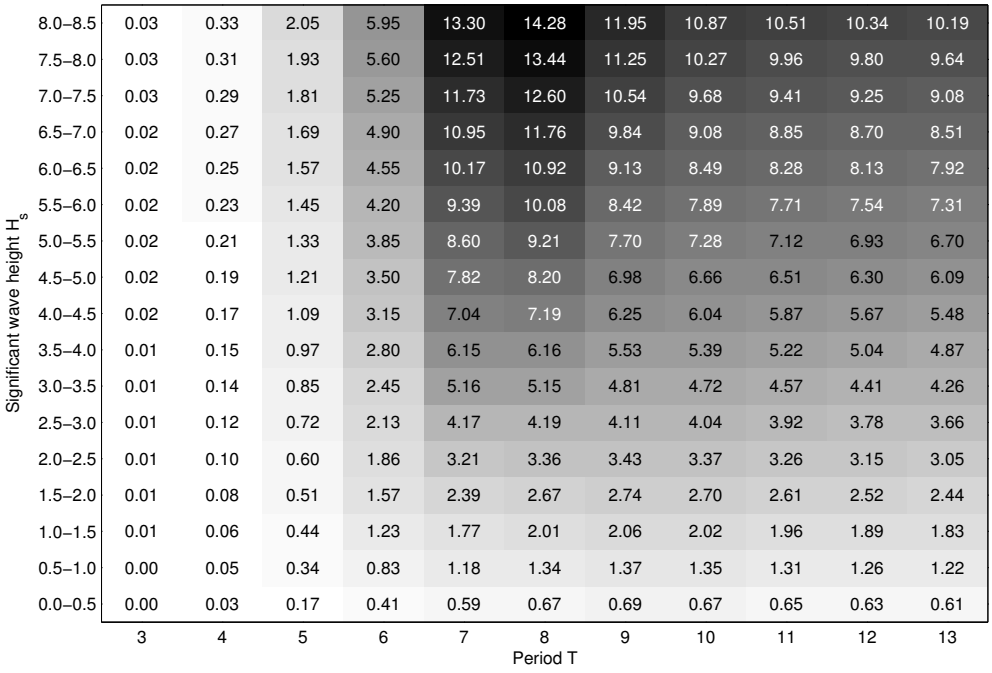

Figure 10: Displacement matrix for a WEC designed to operate in Class 2. The vertical shows significant wave–height (from 0 to 8.5 m), and the horizontal the energy period (from 3 to 13 seconds), while the entries give the significant displacement $\zeta^{1/3}$ in heave in m.

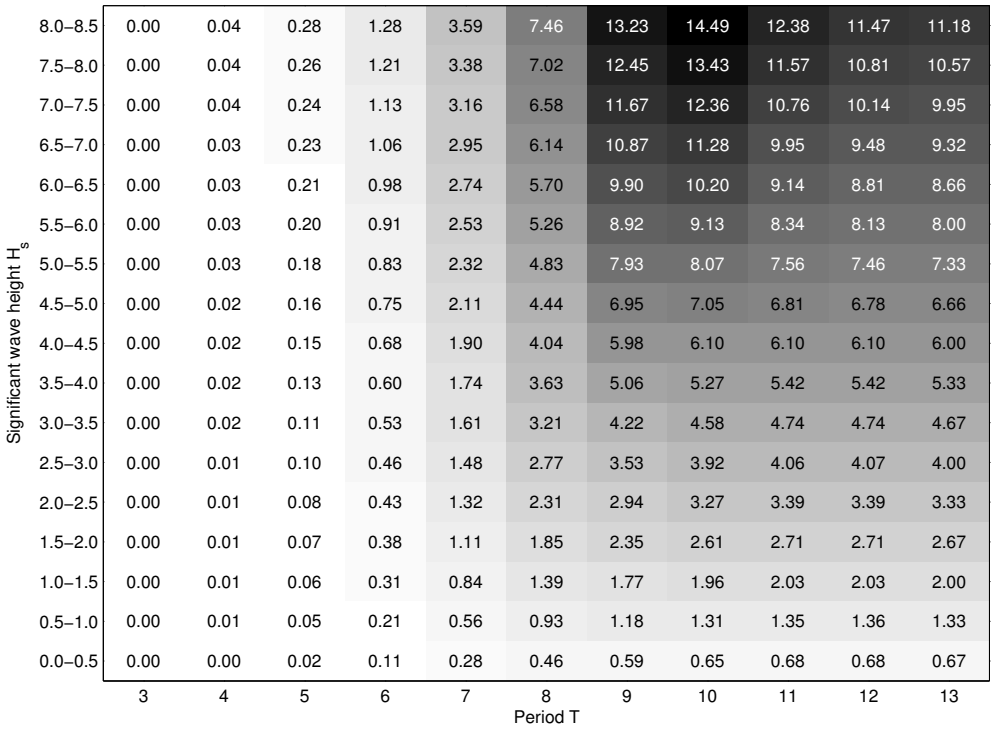

Figure 11: Displacement matrix for a WEC designed to operate in Class 3. The vertical shows significant wave–height (from 0 to 8.5 m), and the horizontal the energy period (from 3 to 13 seconds), while the entries give the significant displacement $\zeta^{1/3}$ in heave in m.

A. (2015). "Wave climate analysis for the design of wave energy harvesters in the Mediterranean Sea." *Renewable Energy*, 77, 125–141.

Berggren, L. and Johansson, M. (1992). "Hydrodynamic coefficients of a wave energy device consisting of a buoy and a submerged plate." *Applied Ocean Research*, 14(1), 51–58.

Black, J. L. and Mei, C. C. (1970). "Scattering and radiation of water waves." MIT Water Resources and Hydrodynamics Lab, Cambridge.

Boccotti, P. (2014). *Wave mechanics and wave loads on marine structures*. Butterworth-Heinemann.

Boccotti, P., Arena, F., Fiamma, V., Romolo, A., and Barbaro, G. (2012). "Small-Scale Field Experiment on Wave Forces on Upright Breakwaters." *Journal of Waterway, Port, Coastal, and Ocean Engineering*, 138(2), 97–114.

Borgarino, B., Babarit, A., and Ferrant, P. (2012). "Impact of wave interactions effects on energy absorption in large arrays of wave energy converters." *Ocean Engineering*, 41, 79–88.

Brodtkorb, P. A., Johannesson, P., Lindgren, G., Rychlik, I., Rydén, J., and Sjö, E. (2000). "WAFO - a Matlab Toolbox for the Analysis of Random Waves and Loads." *Proc. 10'th Int. Offshore and Polar Eng. Conf., ISOPE, Seattle, USA*, Vol. 3, 343–350.

Child, B. F. M. and Venugopal, V. (2010). "Optimal configurations of wave energy device arrays." *Ocean Engineering*, 37(16), 1402–1417.

Coe, R. G. and Neary, V. S. (2014). "Review of Methods for Modeling Wave Energy Converter Survival in Extreme Sea States." *Proceedings of the 2nd Marine Energy Technology Symposium (METS2014)*, Seattle, WA.

Fedele, F. and Arena, F. (2005). "Weakly nonlinear statistics of high random waves." *Physics of Fluids*, 17(2), 1–10.

Garnaud, X. and Mei, C. C. (2009). "Wave-power extraction by a compact array of buoys." *Journal of Fluid Mechanics*, 635, 389–413.

Garnaud, X. and Mei, C. C. (2010). "Comparison of wave power extraction by a compact array of small buoys and by a large buoy." *IET renewable power generation*, 4(6), 519–530.

Goldsmith, V. and Sofer, S. (1983). "Wave Climatology of the Southeastern Mediterranean: An Integrated Approach." *Israel Journal of Earth Sciences*, 32, 1–51.

Hiles, C., Beatty, S., and de Andres, A. (2016). "Wave Energy Converter Annual Energy Production Uncertainty Using Simulations." *Journal of Marine Science and Engineering*, 4(3), 53.

Hiles, C., David, A., Guitierrez, D. A., Beatty, S., Buckham, B., and Bc, V. (2015). "A case study on the matrix approach to WEC performance characterization." *European Wave and Tidal Energy Conference*.

Kofoed, J. and Folley, M. (2016). "Determining Mean Annual Energy Production." *Numerical Modelling of Wave Energy Converters*, Elsevier, 253–266.

Kroszynski, U. I. and Stiassnie, M. (1978). "Deep water wave distribution based on Ashdod data." Coastal & Marine Engineering Research Institute, Haifa.

Kroszynski, U. I. and Stiassnie, M. (1979). "Wave power estimates on Eastern Mediterranean coast." *Journal of the Energy Division, ASCE*, 105(EY1), 159–164.

Maisondieu, C. (2015). "WEC survivability threshold and extractable wave power." *Proceedings of the 11th European Wave and Tidal Energy Conference*.

Peckolt, J., Lucas, J., Jan, P., and Friedhoff, B. (2015). "Cable robots for experimental investigations of wave energy converters." *Proceedings of the 11th European Wave and Tidal Energy Conference*, 1–7.

Romolo, A. and Arena, F. (2008). "Mechanics of nonlinear random wave groups interacting with a vertical wall." *Physics of Fluids*, 20(3).

Rosen, D. S. and Kit, E. (1982). "Evaluation of the Wave Characteristics at the Mediterranean Coast of Israel." *Israel Journal of Earth Sciences*, 30, 120–134.

Starling, M. (2009). "Guidelines for Reliability, Maintainability and Survivability of Marine Energy Conversion Systems." The European Marine Energy Center Ltd.

Teillant, B., Costello, R., Weber, J., and Ringwood, J. (2012). "Productivity and economic assessment of wave energy projects through operational simulations." *Renewable Energy*, 48, 220–230.

Wu, B., Wang, X., Diao, X., Peng, W., and Zhang, Y. (2014). "Response and conversion efficiency of two degrees of freedom wave energy device." *Ocean Engineering*, 76, 10–20.

Xu, D., Stuhlmeier, R., and Stiassnie, M. (2017). "Harnessing wave power in open seas II: very large arrays of wave-energy converters for 2D sea states." *Journal of Ocean Engineering and Marine Energy*, 3(2), 151–160.